NASA Technical Memorandum 86661

Airborne Astronomy Program
Medium Altitude Missions Branch
Preprint Series 025

The Jovian Atmospheric Window at 2.7 μm: A Search for H_2S

Harold P. Larson, D. Scott Davis,
Reiner Hofmann, and
Gordon L. Bjoraker

November 1984

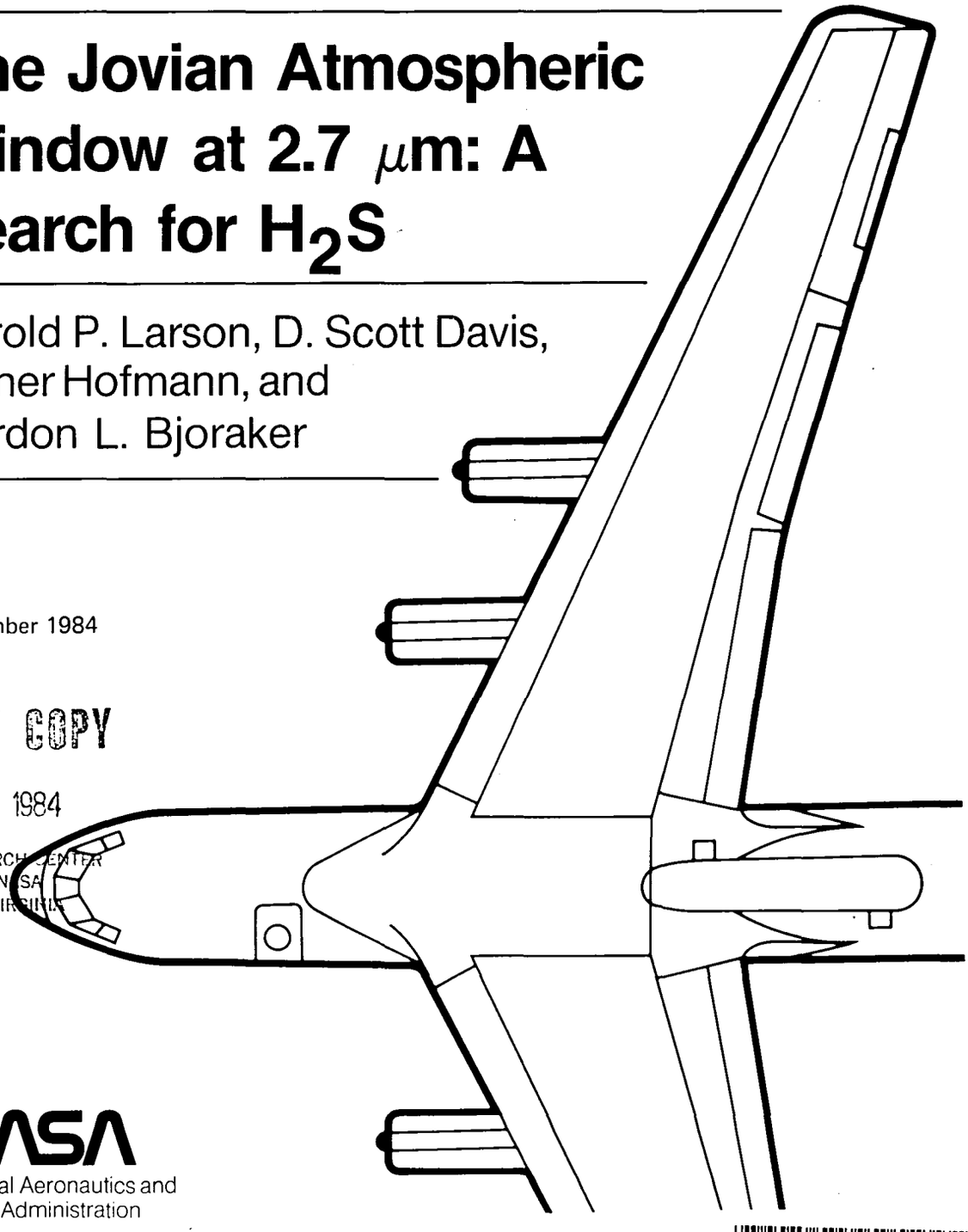

National Aeronautics and
Space Administration

NASA Technical Memorandum 86661

Airborne Astronomy Program
Medium Altitude Missions Branch
Preprint Series 025

The Jovian Atmospheric Window at 2.7 μm: A Search for H_2S

Harold P. Larson,
D. Scott Davis, University of Arizona, Tuscon, Arizona
Reiner Hofmann, Max-Planck-Institute fur Physik und Astrophysik, Munich, Germany
Gordon L. Bjoraker, University of Arizona, Tucson, Arizona

November 1984

National Aeronautics and
Space Administration

Ames Research Center
Moffett Field, California 94035

The Jovian Atmospheric Window at 2.7 μm: A Search for H_2S

by

Harold P. Larson
Lunar and Planetary Laboratory
University of Arizona
Tucson, Arizona 85721

D. Scott Davis
Steward Observatory
University of Arizona
Tucson, Arizona 85721

Reiner Hofmann
Max-Planck-Institut für Physik und Astrophysik
Institut für Extraterrestriche Physik
8046 Garching bei München
Federal Republic of Germany

Gordon L. Bjoraker
Department of Planetary Sciences
University of Arizona
Tucson, Arizona 85721

Running Title: Search for H_2S on Jupiter

Send all correspondence to: Harold P. Larson
Lunar and Planetary Laboratory
University of Arizona
Tucson, AZ 85721

ABSTRACT

We have observed the atmospheric transmission window at 2.7 μm in Jupiter's atmosphere at a spectral resolution of 0.1 cm^{-1} from the Kuiper Airborne Observatory. From our analysis of the CH_4 abundance (∿ 80 m-am) and the H_2O abundance (< 0.0125 cm-am) we determined that the penetration depth of solar flux at 2.7 μm is near the base of the NH_3 cloud layer. Our upper limit to H_2O at 2.7 μm and other recent results suggest that photolytic reactions in Jupiter's lower troposphere may not be as significant as was previously thought. Our search for H_2S in Jupiter's atmosphere yielded an upper limit of ∿ 0.1 cm-am. The corresponding limit to the elemental abundance ratio [S]/[H] was ∿ 1.7×10^{-8}, about 10^{-3} times the solar value. Upon modeling the abundance and distribution of H_2S in Jupiter's atmosphere we concluded that, contrary to expectations, sulfur-bearing chromophores are not present in significant amounts in Jupiter's visible clouds. Rather, it appears that most of Jupiter's sulfur is locked up as NH_4SH in a lower cloud layer. Alternatively, the global abundance of sulfur in Jupiter may be significantly depleted.

I. INTRODUCTION

Jupiter is one of the most intensively studied objects in astronomy, but several regions of its spectrum remain poorly explored because of telluric interference at ground-based observatories and various technical limitations to the use of spectrometers on aircraft, balloons and spacecraft. In this paper we report the first very high resolution observations of Jupiter's atmospheric transmission window at 2.7 μm (see Fig. 1 in Ridgway et al. (1976) for an overview of Jupiter's ir spectrum). Our analysis concentrates on the search for certain key trace constituents that relate to Jovian atmospheric chemistry, particularly the poorly characterized cloud chromophores.

The Jovian window at 2.7 μm is completely obscured by telluric CO_2 and H_2O absorptions at all ground-based telescopes. Observations must therefore be conducted from special high altitude facilities. The few successful efforts are summarized in Fig. 1. This spectral window was first revealed by Danielson (1966) using a low resolution ($\sim$ 70 cm^{-1}) balloon-borne prism spectrometer (Fig. 1a). He attributed the presence and shape of this window to strong H_2, CH_4, and NH_3 absorptions on Jupiter. In 1978 we conducted higher resolution exploratory observations of this window with a Fourier spectrometer at the Kuiper Airborne Observatory (KAO). These data, displayed in Fig. 1b at 10 cm^{-1} resolution, reveal the detailed shape of the Jovian continuum across this window. Drossart and Encrenaz (1983) used this envelope to assess the diagnostic value of lower resolution ($\sim$ 30 cm^{-1}) observations of this spectral region on Jupiter from Galileo. As expected, searches for new trace atmospheric constituents on Jupiter are futile at such low resolution. The spectrum in Fig. 1c is an excerpt from our new airborne spectrum of Jupiter at 2.7 μm. Its very high spectral

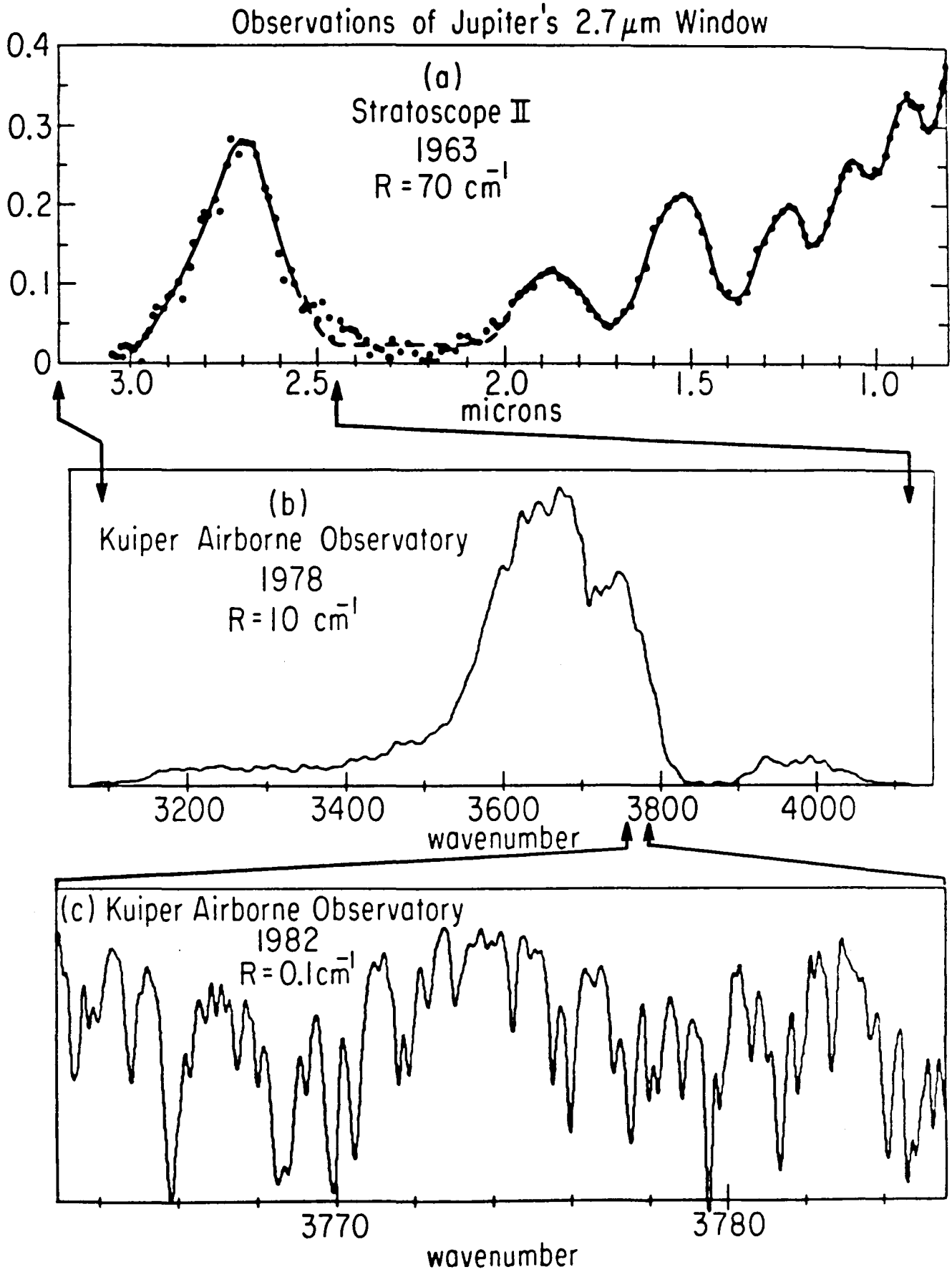
Observations of Jupiter's 2.7 μm Window
(a)
Stratoscope II
1963
R = 70 cm⁻¹
0.4
0.3
0.2
0.1
0
3.0
2.5
2.0
1.5
1.0
microns
(b)
Kuiper Airborne Observatory
1978
R = 10 cm⁻¹
3200
3400
3600
3800
4000
wavenumber
(c) Kuiper Airborne Observatory
1982
R = 0.1 cm⁻¹
3770
3780
wavenumber

Figure 1

resolution ($\sim$0.1 cm^{-1}) allows sensitive searches for numerous trace constituents, including several important molecules such as H_2S and HF that do not have strong bands coincident with other windows in Jupiter's ir spectrum.

II. OBSERVATIONS

We observed Jupiter on March 9 and 11, 1982 (UT) from the KAO with a high resolution Fourier spectrometer (Davis et al., 1980). The unapodized resolution was 0.0975 cm^{-1} and the spectral bandpass was 3300-4700 cm^{-1}. Thermal background flux accompanying the planetary signal was removed by use of the two complementary input beams of the spectrometer. Two steps were involved: simultaneous illumination of both inputs with background flux, thereby eliminating most background in real-time; and periodic switching of the planet between the inputs, which provided for cancellation of residual background levels during data processing. We also recorded lunar comparison spectra to calibrate instrumental response and to locate telluric absorptions.

At the time of our observations the Doppler shift of Jovian absorption lines was +0.28 cm^{-1} (blue shift) at 3700 cm^{-1}. This is almost three times the instrumental line width, thus permitting clean separation of terrestrial and planetary absorptions formed by the same species (e.g. H_2O). Jupiter's angular diameter was 42 arcsec, of which the central 17 arcsec was admitted to the spectrometer. Because of Jupiter's rapid rotation, the Doppler broadening of spectral lines in this field-of-view was about 0.07 cm^{-1}, slightly less than the instrumental resolution limit.

During the observations the altitude of the KAO was maintained constant at 12.5 km. The average line-of-sight residual water vapor abundance was only

about 7 μm precipitable H_2O, a value obtained by fitting synthetic H_2O spectra to the lunar data. In our experience this is a rather low value for this altitude, suggesting ideal atmospheric conditions for these observations (low tropopause; cold, dry stratosphere). This does not mean, however, that the planetary data are free from telluric interference. In fact, residual terrestrial absorption severely limits the interpretation of much of Jupiter's 2.7-μm spectrum. This problem is illustrated in the high altitude lunar comparison spectra of Fig. 2. Even at low resolution (10 cm^{-1}, Fig. 2a) telluric CO_2 and H_2O show significant absorption in the 2.7-μm region where the Jovian flux peaks. These terrestrial features appear to have been successfully removed in the low resolution Jovian ratio spectrum in Fig. 1b, but the true situation is revealed at high resolution in Figs. 2b and 2c. Saturated CO_2 and H_2O lines block significant amounts of Jovian flux and no numerical processing of the data can restore a semblance of continuity to Jupiter's high resolution 2.7-μm spectrum.

It is not possible to display the entire high resolution spectrum of Jupiter's 2.7-μm window in this paper. We therefore present in the next section an overview of this spectral window, thereby demonstrating its potential for trace constituent analyses. The discussion also includes our estimate of the approximate depth of spectral line formation in Jupiter's atmosphere at 2.7 μm. This level is compared to current cloud models of Jupiter's troposphere to establish a perspective for interpreting our abundance limits.

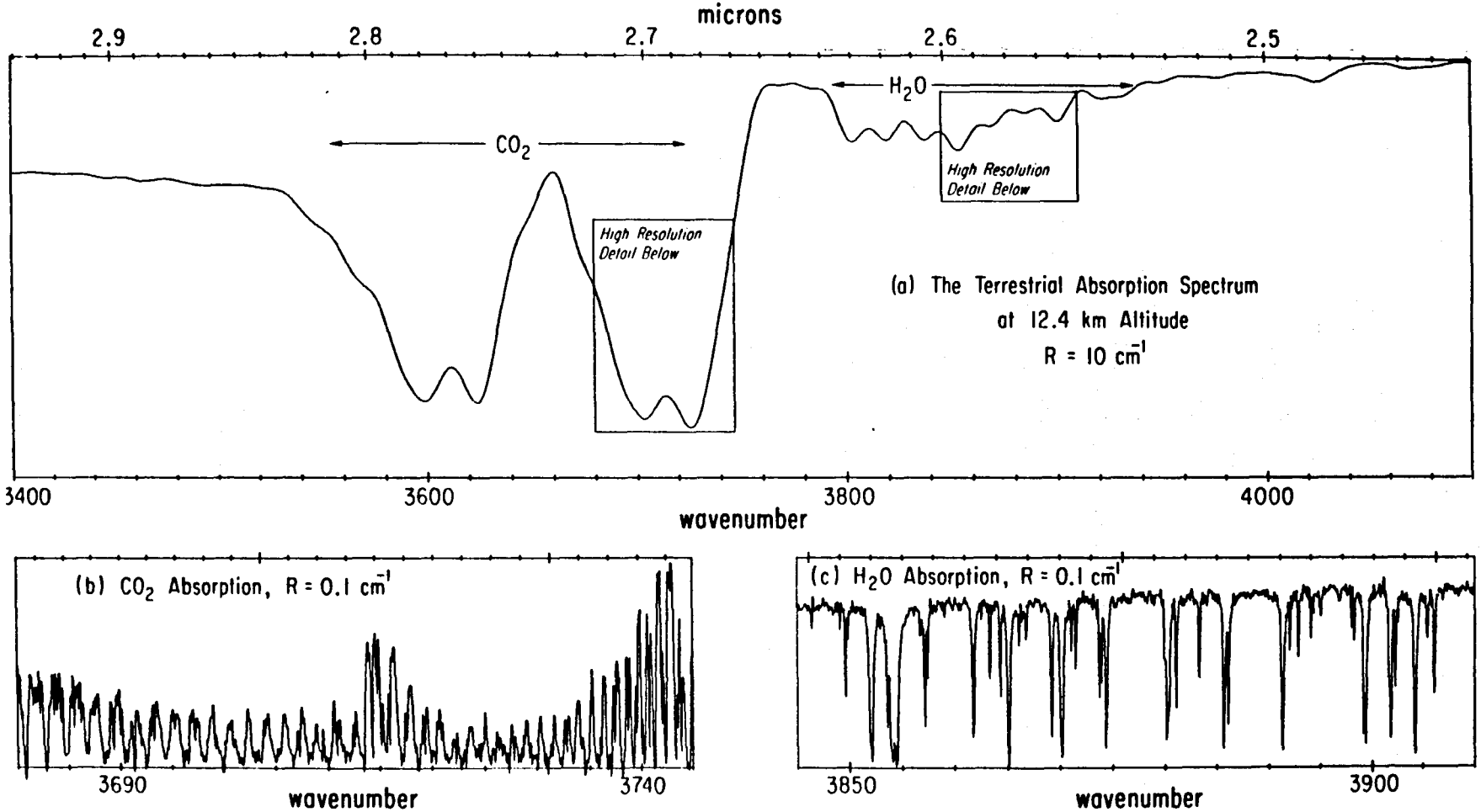
microns
2.9
2.8
2.7
2.6
2.5
H_2O
CO_2
High Resolution Detail Below
High Resolution Detail Below
(a) The Terrestrial Absorption Spectrum at 12.4 km Altitude R = 10 cm^{-1}
3400
3600
3800
4000
wavenumber
(b) CO_2 Absorption, R = 0.1 cm^{-1}
3690
3740
wavenumber
(c) H_2O Absorption, R = 0.1 cm^{-1}
3850
3900
wavenumber

Figure 2

III. OVERVIEW OF JUPITER'S 2.7 μm WINDOW

Major absorptions. In Fig. 3 we compare the low resolution profile of Jupiter's 2.7-μm window with spectra of those constituents (H_2, CH_4, NH_3) whose strong absorptions shape this spectral region. Methane and NH_3 establish the long wavelength side of this window. At about 3150 cm^{-1} CH_4 becomes transparent, but NH_3 continues to absorb strongly until about 3500 cm^{-1}, thus producing the broad, flat region of absorption from 3100-3500 cm^{-1} in Jupiter's spectrum. Hydrogen and CH_4 terminate the short wavelength side of the planetary window. At 3750 cm^{-1} CH_4 begins to absorb strongly again, reaching saturation at 3850 cm^{-1} and then yielding a narrow region of transmission from 3900-4050 cm^{-1}. Also, the pressure-induced spectrum of H_2 produces rapidly decreasing transmission between 3900-4100 cm^{-1}. Below 3100 cm^{-1} the next region of transmission in Jupiter's atmosphere begins at about 2200 cm^{-1}, the "5-μm" window. Above 4100 cm^{-1} the next region of planetary flux begins around 4800 cm^{-1}, which is itself a poorly studied window because of terrestrial H_2O absorption. Thus, between 2-5 μm there exists only this very narrow region from 3150-4100 cm^{-1} where simultaneous high transmission in H_2, CH_4 and NH_3 create a relatively rare opportunity in the near-ir to probe Jupiter's atmosphere for other constituents.

The room temperature laboratory comparison spectra of CH_4 and NH_3 in Fig. 3 closely simulate the continuum spectral characteristics of Jupiter's 2.7 μm window. However, these laboratory abundances may not be the actual values appropriate for Jupiter's atmosphere. The interpretive problems are well known from analyses of Jupiter's spectrum at other wavelengths. First, on the reasonable assumption that the spectral line forming region at 2.7 μm

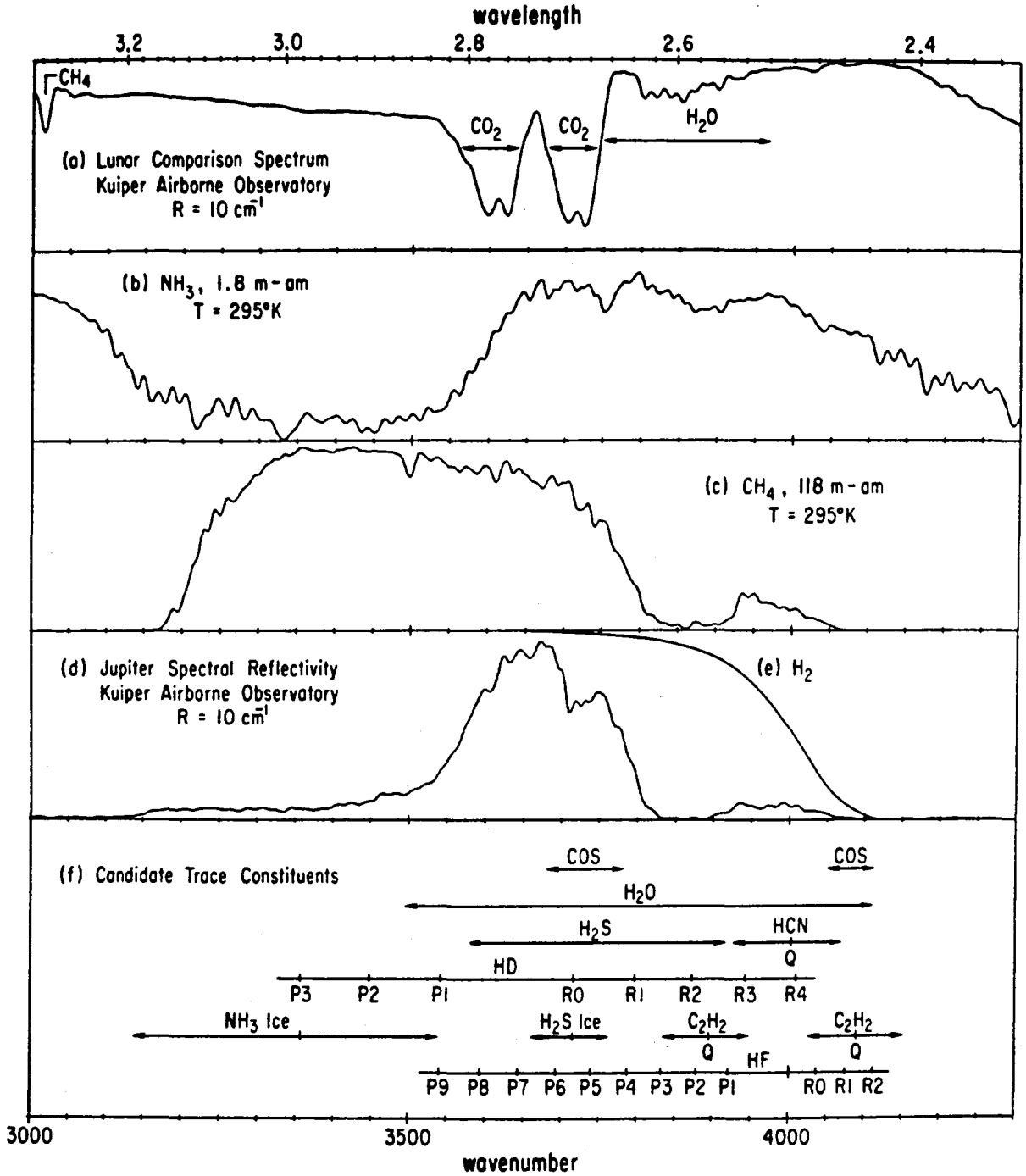
wavelength
3.2
3.0
2.8
2.6
2.4
CH4
CO2
CO2
H2O
(a) Lunar Comparison Spectrum
Kuiper Airborne Observatory
R = 10 cm-1
(b) NH3, 1.8 m-am
T = 295°K
(c) CH4, 118 m-am
T = 295°K
(d) Jupiter Spectral Reflectivity
Kuiper Airborne Observatory
R = 10 cm-1
(e) H2
(f) Candidate Trace Constituents
COS
COS
H2O
H2S
HCN
Q
HD
P3 P2 P1 R0 R1 R2 R3 R4
NH3 Ice
H2S Ice
C2H2
Q
C2H2
Q
HF
P9 P8 P7 P6 P5 P4 P3 P2 P1 R0 R1 R2
3000
3500
4000
wavenumber

Figure 3

is somewhere in Jupiter's troposphere ($T \sim 175°K$), room temperature laboratory data do not provide correct relative intensities for comparison with the planetary data. Also, these spectra do not simulate the effects of scattering in real planetary atmospheres. Because of these limitations we do not present the laboratory spectra in Fig. 3 as rigorous fits to the Jovian data. Rather, we use this composite to confirm Danielson's original expectations that H_2, CH_4, and NH_3 alone are sufficient to account for the shape of this planetary window. That is, we see no features in Jupiter's ratio spectrum in Fig. 3d that can be assigned unequivocally to new gaseous species. Of course, much more stringent tests for trace gaseous constituents are possible with our new high resolution data. We review some of the possibilities below.

Candidate trace constituents. In Fig. 3f we identify molecules having prominent absorption features coincident with at least part of Jupiter's 2.7-μm window. All of the species are expected to be relevant to some aspect of Jovian atmospheric chemistry. The near-ir vibration-rotation bands of these candidates differ widely in appearance. The diatomic species have only a very few, widely spaced transitions, each of which is marked in Fig. 3f. The complex spectra of H_2O and H_2S display hundreds of irregularly spaced transitions; the arrows in Fig. 3f indicate the spectral bandwidth over which these transitions occur. If the spectrum includes a Q-branch, which permits an especially sensitive test for trace constituents, its position is marked in Fig. 3f with the symbol Q. This paper deals specifically with the search for H_2S on Jupiter; the other candidate species will be treated in subsequent analyses.

The spectral resolution of 10 cm^{-1} in Fig. 3d is ideal for revealing absorptions by solids, especially ices of known or candidate species. We therefore include in Fig. 3f several condensates having solid state absorptions coincident with Jupiter's 2.7-μm spectrum. The strongest absorption by NH_3

ice in the near-ir occurs between 3100-3500 cm^{-1}; its absorption coefficient peaks at 3374 cm^{-1} (Sill et al., 1980). This spectrum of NH_3 ice coincides with strong absorption by gaseous NH_3. Both phases are compatible with the broad, flat absorption between 3100-3500 cm^{-1} in Jupiter's spectrum in Fig. 3d. However, it may be significant that Jupiter's spectral reflectivity in this region is appreciably smoother than that of the laboratory comparison spectrum of gaseous NH_3 (compare Fig. 3b with Fig. 3d from 3100-3500 cm^{-1}). Certainly, the saturated gaseous NH_3 feature at 3330 cm^{-1} should have registered in Jupiter's spectrum if the gaseous phase alone constituted the opacity source in this spectral region. We therefore suspect that the relatively featureless spectrum of solid NH_3 contributes to the long wavelength side of Jupiter's 2.7-μm window.

The broad feature from 3700-3750 cm^{-1} in Jupiter's spectrum in Fig. 3d has several possible interpretations. It could be merely residual terrestrial CO_2 because of air mass mismatch, although we would then expect a similar feature at the position of the neighboring CO_2 band. Alternatively, it could be a superposition of weak NH_3 and CH_4 lines that do not appear prominently in room temperature laboratory data. However, at high spectral resolution we do not see any evidence for strong Jovian gaseous absorptions in this spectral region. This suggests again the possibility of absorption by a solid. The Jovian feature from 3700-3750 cm^{-1} is coincident with the strongest near-ir absorption of solid H_2S (Ferraro and Fink, 1977), but we discount this possibility because H_2S should not condense anywhere in Jupiter's atmosphere (see Section IV). However, there is a very weak feature in the spectrum of solid NH_3 in the region around 3725 cm^{-1} (Sill et al., 1980) that may appear more prominently in a scattering environment. Much additional research is required to confirm this

possibility and that noted above for solid NH_3 absorption from 3100-3500 cm^{-1}. We will therefore defer any further discussion of Jupiter's NH_3 spectrum at 2.7 μm to a future paper.

Line forming region. For wavelengths less than 2 μm Jupiter's spectrum is produced by reflected solar flux, while at 5 μm and beyond the spectrum is due to thermal emission. The 2.7-μm window is therefore in a transition region, although simple calculations establish that Jupiter's 2.7-μm signal will be dominated by reflected solar flux for an albedo of $\sim$ 0.3 and T < 200°K in the line forming region. Only observations of Jupiter's dark side from a spacecraft will detect the much weaker thermal signal from Jupiter at 2.7 μm. We therefore expect that the mechanism of spectral line formation at 2.7 μm will be similar to that deduced from observations at shorter wavelengths (0.6-1.6 μm). That is, it should be confined to depths that are constrained from above by scattering in the upper troposphere and from below by reflection from cloud layers in the lower troposphere.

We adopt in Fig. 4 the tropospheric cloud model from Bjoraker (1984) as a reasonable consensus of current opinions concerning Jupiter's vertical atmospheric structure. This picture represents numerous refinements to early cloud models that required at least two distinct layers to satisfy spectral observations (Danielson and Tomasko, 1969) and thermochemical expectations (Lewis, 1969a). Key features of the model atmosphere include an NH_3 cloud whose base is near P = 0.75 bar and T = 150°K and a thicker cloud of variable 5 μm opacity (τ = 1-4) at the P = 2.0 bars, T = 206°K level. Bjoraker (1984) rejects the necessity of including a third cloud layer at P$\sim$ 6 bars because H_2 gas opacity alone fits the 5 μm observations that originate at such depths in Jupiter's atmosphere. The optical thickness τ associated with the clouds in Fig. 4 refers to attenuation

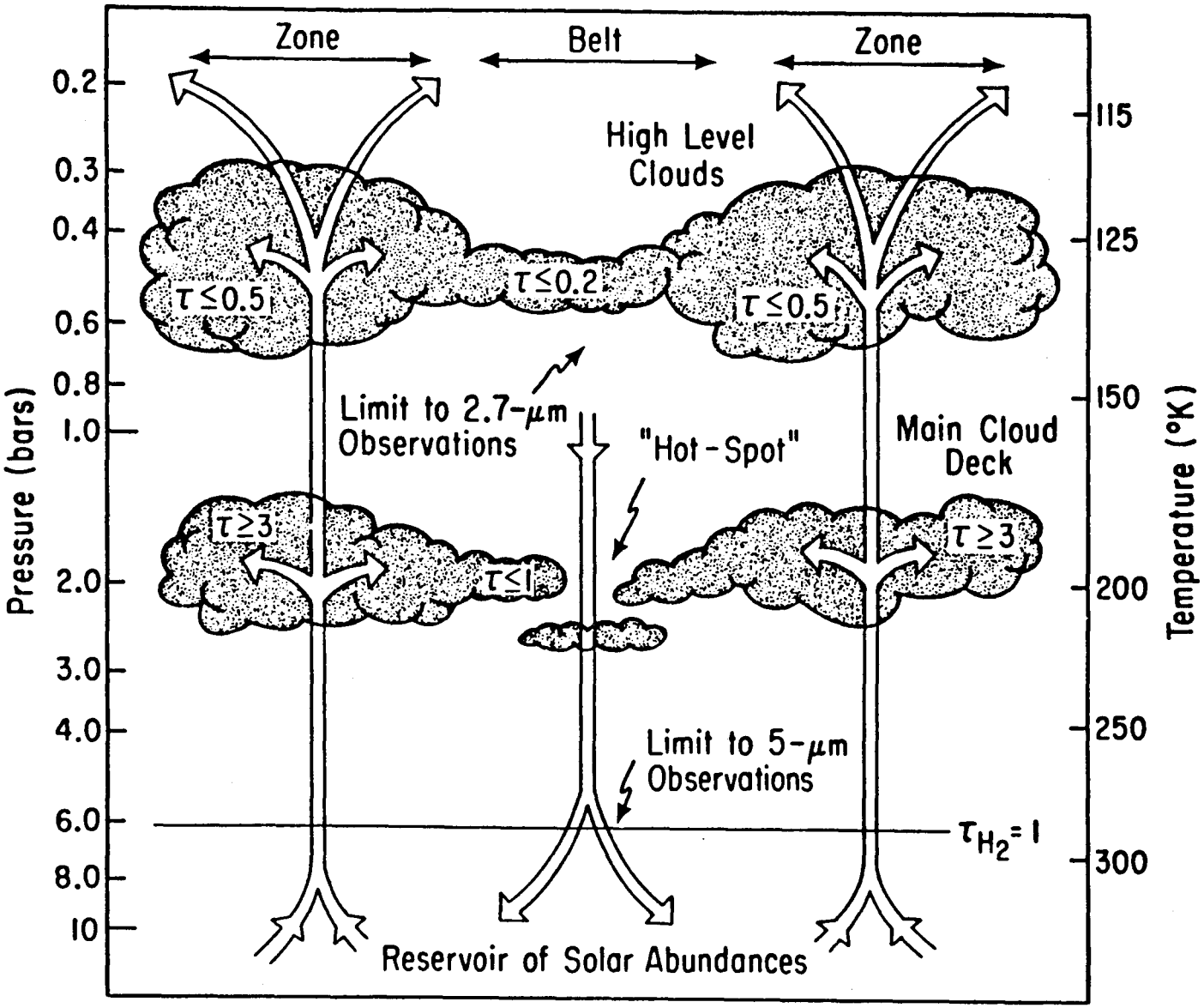
Zone
Belt
Zone
High Level
Clouds
τ≤0.5
τ≤0.2
τ≤0.5
Limit to 2.7-μm
Observations
"Hot-Spot"
Main Cloud
Deck
τ≥3
τ≤1
τ≥3
Limit to 5-μm
Observations
$\tau_{H_2}=1$
Reservoir of Solar Abundances
Pressure (bars)
0.2
0.3
0.4
0.6
0.8
1.0
2.0
3.0
4.0
6.0
8.0
10
115
125
150
200
250
300
Temperature (°K)

Figure 4

of planetary thermal emission at 5 μm. However, there is a significant change in physics between one-way transmission of thermal flux at 5 μm and two-way transmission of reflected solar radiation at shorter wavelengths. In particular, the relatively small values for τ in the high level clouds in Fig. 4 do not guarantee significant penetration of this layer by near-ir or visible solar photons. This point is very important for our spectral analysis. Rather than adopt either the long wavelength or short wavelength picture, we present later in this section our independent estimate of the penetration depth of solar photons at 2.7 μm using Jovian CH_4 and H_2O spectral features.

The horizontal cloud structure indicated schematically in Fig. 4 refers to Jupiter's visible morphology. In general, regions designated as zones are characterized by light-colored cloud bands and relatively cold effective 5-μm brightness temperatures ($T_{BB} \sim 200°K$). Belts, on the other hand, are typically warmer (T_{BB} up to 265°K) and darker in color. Since our spectrometer's field-of-view included both belts ($\sim$ 55%) and zones ($\sim$ 45%), our 2.7-μm Jovian spectrum represents an areal average of these morphologically distinct areas. In general, belts are considered the best locations to study lower levels in Jupiter's atmosphere. The upper clouds in the belts are often described as optically thin or even absent, whereas thicker clouds in the zones limit observations of deeper levels. This picture has supported models in which solar flux penetrates the gap between the cloud layers in the belts (e.g. Sato and Hansen, 1979), including uv photons for photochemical processing of material in the lower cloud layer (Lewis and Prinn, 1970). Some aspects of this picture seem to require substantial revision. We discuss in Section V how our interpretation of Jupiter's 2.7-μm spectrum and other recent studies indicate that there may be a significantly diminished role for solar flux in Jupiter's lower troposphere, even in the belts.

For additional details concerning Jupiter's atmospheric structure, the following references should be consulted: Sato and Hansen (1979) for a presentation of two-cloud scattering models based upon ground-based observations; Owen and Terrile (1981) for a description of Jupiter's clouds in terms of Voyager imagery; Terrile and Westphal (1977) for an analysis of Jupiter's clouds using ground-based images at 5 μm; Marten et al. (1981) for a description of the upper cloud layer from Voyager ir spectroscopy; and Bezard et al. (1983) and Bjoraker (1984) for analyses of Jupiter's lower cloud layers from Voyager ir spectroscopy.

We use the known Jovian constituents CH_4 and H_2O to set numerical limits to the line forming region at 2.7 μm. Methane absorption is prominent throughout Jupiter's 2.7-μm spectrum, and its abundance will not be affected by saturation or chemical depletion in Jupiter's troposphere. However, its suitability for quantitative abundance measurements is limited by the current lack of laboratory analyses appropriate to Jovian atmospheric conditions. Water vapor is potentially a very sensitive probe of vertical penetration because its abundance is controlled by saturation in Jupiter's upper troposphere. The 2.7-μm H_2O bands have been analyzed, so synthetic spectra can be calculated for realistic comparisons with the planetary data. However, the use of H_2O as a vertical probe is limited by still-unanswered questions concerning its global abundance in Jupiter and differences between belt and zone distributions. Within these limitations we summarize below how both molecules set limits to the depth of penetration of solar flux at 2.7 μm on Jupiter.

As noted above, the low resolution laboratory spectrum of CH_4 in Fig. 3c fits the continuum spectral characteristics of Jupiter's 2.7 μm window. That is, for wavenumbers greater than 3600 cm^{-1} it reproduces the regions of high albedo, total saturation, and the transition regions connecting these two limits.

At high spectral resolution the individual CH_4 lines present a more confusing picture. Line-to-line mismatches in intensities between the planetary and laboratory spectra are probably due to temperature effects. A range of abundances from 75-250 m-am is indicated if these room temperature laboratory spectra are used literally at either high or low spectral resolution. However, without corrections for temperature and line broadening these values are probably underestimated. We therefore adopt a CH_4 abundance of 200 m-am as a provisional fit to Jupiter's 2.7-μm spectrum. If referred to a reflecting layer model, the CH_4 abundance for a one-way transmission is 80 m-am for an air mass factor of 2.5. This value is consistent with measurements of strong CH_4 bands elsewhere in the near-ir (52 m-am, de Bergh et al., 1976), but lower than values from weak CH_4 bands (150 m-am, Lutz et al., 1976; 130 m-am, Fink and Larson, 1979). Our 2.7-μm Jovian CH_4 abundance indicates a line forming region whose base is at $P \sim 0.75$ bar, $T \sim 150°K$ using Bjoraker's tropospheric composition model (1984). According to Fig. 4 this is just at the base of the upper cloud layer.

Water vapor was readily detected in high altitude spectra of Jupiter at 5 μm (Larson et al., 1975). At 2.7 μm, however, we find no evidence for Jovian H_2O in spite of optimized spectroscopic conditions for detection. We used two techniques to search for H_2O: a line-by-line examination for Doppler-shifted Jovian companions to telluric lines; and a cross-correlation of Jupiter's spectrum with synthetic spectra of H_2O. The results are discussed below.

In Fig. 5a we display a section of Jupiter's spectrum that includes a strong, isolated H_2O line at 3759.8 cm^{-1}. This saturated H_2O line is telluric in origin, as demonstrated by its presence in the lunar spectrum in Fig. 5b, and it represents an abundance of about 7 μm precipitable H_2O. The H_2O abundance detected on Jupiter at 5 μm was about 100 μm precipitable H_2O, an amount that masked the terrestrial lines. Clearly, this is not the situation

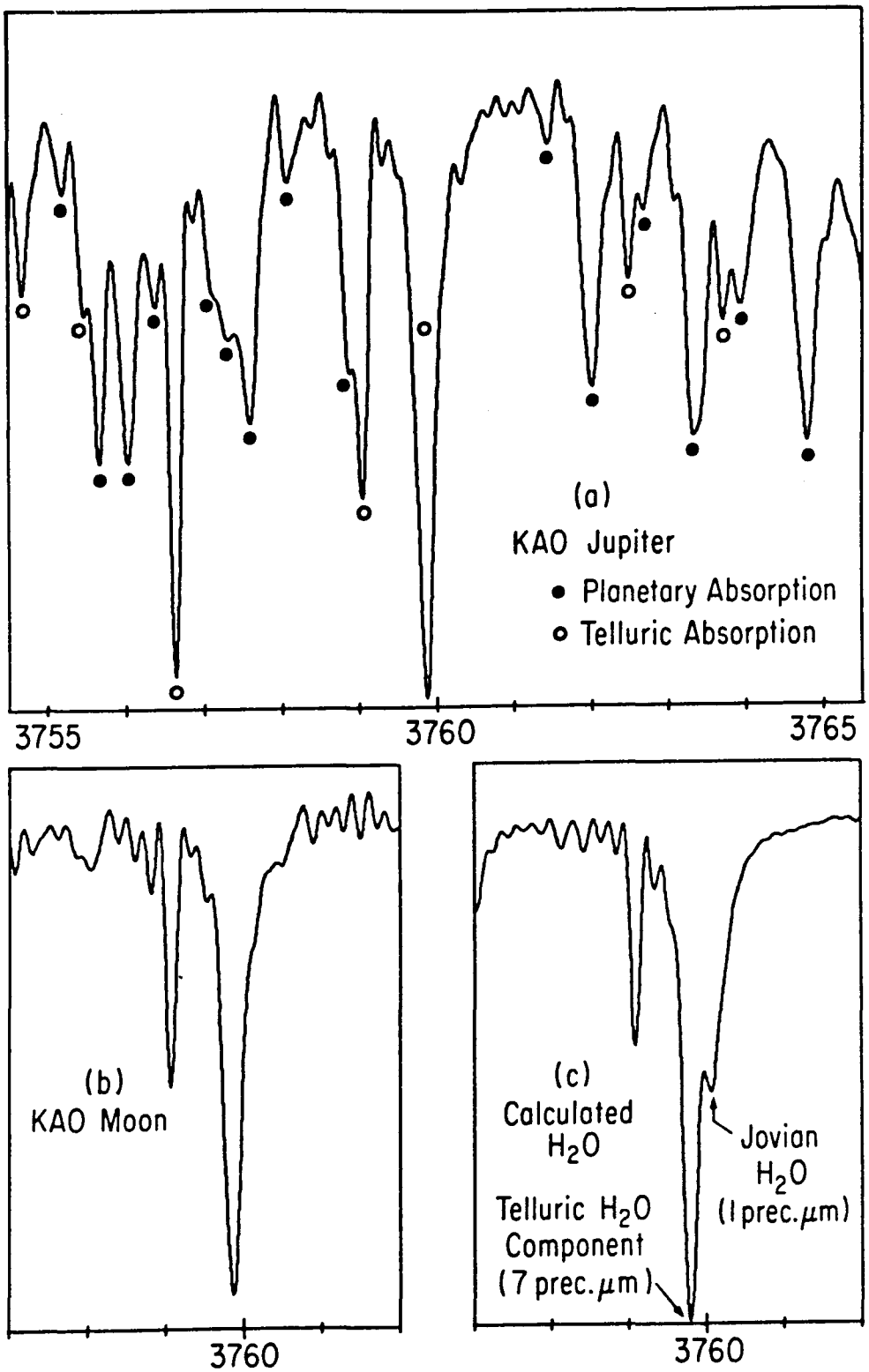
(a)
KAO Jupiter
Planetary Absorption
Telluric Absorption
3755
3760
3765
(b)
KAO Moon
3760
(c)
Calculated
H_2O
Telluric H_2O
Component
(7 prec.μm)
Jovian
H_2O
(1 prec.μm)
3760

Figure 5

at 2.7 μm. However, the large Doppler shift (+0.28 cm^{-1}) compared to the spectral resolution (0.1 cm^{-1}) permits tests for Jovian H_2O abundances that are substantially less than the residual terrestrial concentration above the KAO. This is illustrated in Fig. 5c with a synthetic H_2O spectrum fit to the KAO lunar spectrum. This calculation includes a Doppler-shifted Jovian component with an abundance of 1 μm precipitable H_2O. This small amount appears as a resolved companion on the short wavelength side of the telluric H_2O profile. Upon comparing the calculated profile in Fig. 5c with the observed profile on Jupiter at 3759.8 cm^{-1} in Fig. 5a, we see no evidence for Jovian H_2O at the level of 1 μm precipitable H_2O. Similar conclusions apply to visual inspection of other H_2O lines in the planetary data. If we then use synthetic H_2O spectra calculated for progressively smaller values of the hypothetical Jovian component, we can set a quantitative upper limit to the Jovian H_2O abundance that would still be detectable by visual inspection of the base of the telluric line profile. This limit is about 0.25 μm precipitable H_2O.

An alternative approach, cross-correlation analysis, has the advantage of employing simultaneously all H_2O lines, not just those few isolated transitions amenable to visual inspection. We summarize the results of this procedure with the correlograms in Fig. 6. The autocorrelation of the synthetic spectrum of H_2O without a Jovian component establishes the basic signature of the method (Fig. 6c). A similar profile results (Fig. 6b) when this synthetic spectrum is cross-correlated with the lunar spectrum. When the synthetic H_2O spectrum is cross-correlated with the Jovian spectrum (Fig. 6a), there should be at least an H_2O signature similar to that in Figs. 6b and 6c. This is evident in Fig. 6a, but the result merely confirms that the telluric H_2O spectrum is present in the planetary spectrum. If, however, there were

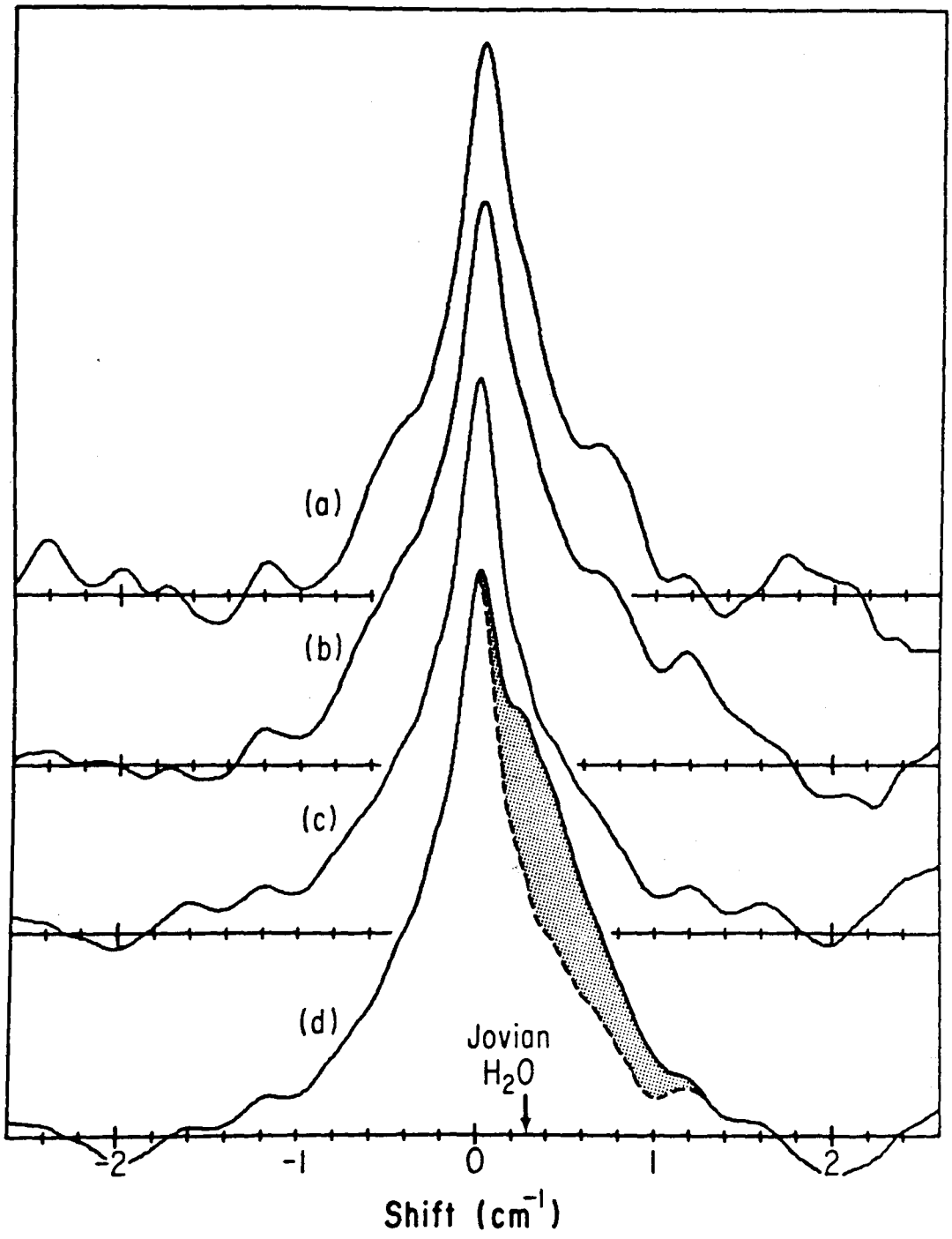

Figure 6

in addition a Doppler-shifted Jovian H_2O component in our planetary spectrum, it would appear in Fig. 6a as an asymmetric broadening of the correlogram. The effect is illustrated in Fig. 6d with the cross-correlation of two synthetic H_2O spectra, one of which contained a Doppler-shifted component with an abundance of 1 μm precipitable H_2O as in Fig. 5c. The obvious asymmetry of the correlogram in the direction of the Doppler shift, indicated by the shaded area, is an alternative way of recognizing weak Jovian H_2O absorption. However, after careful inspection of the cross-correlation of spectra of Jupiter and H_2O in Fig. 6a we see no asymmetric broadening toward shorter wavelengths. This effect was also calibrated to produce a numerical upper limit to H_2O on Jupiter at 2.7 μm. This value is about 0.25 μm precipitable H_2O.

Thus, our two methods for examining Jupiter's 2.7-μm spectrum for H_2O absorption yield the same upper limit: 0.25 μm precipitable H_2O. Expressed as a one-way transmission the Jovian H_2O abundance limit is 0.10 μm precipitable H_2O, or 0.0125 cm-am. From Bjoraker's tropospheric composition model this abundance implies an atmospheric level no deeper than $P \sim 1.2$ bars, $T \sim 176°K$. According to Fig. 4, this limit is well above the tops of the lower clouds. The actual level of line formation could be anywhere above this limit.

In summary, our CH_4 and H_2O analyses constrain the spectral line forming region at 2.7 μm to levels between $P \sim$ 0.75-1.2 bars and $T \sim$ 150-175°K. With reference to Fig. 4, this range includes mid-tropospheric levels between the two Jovian cloud layers. That is, we anticipate that, at least over the belts, some fraction of the reflected solar flux at 2.7 μm may have probed the relatively clear space between the clouds. A rigorous defense of this expectation requires elaborate modeling of the upper cloud layer, including belt-to-zone variations in opacity, and better laboratory comparison data than now exist. For purposes of reporting upper limit determinations in this paper

we adopt the base of the upper cloud layer as a conservative limit to the penetration of solar flux into Jupiter's troposphere at 2.7 μm. The hydrogen abundance corresponding to this level is $\sim 3.0 \times 10^6$ cm-am.

IV. SEARCH FOR H_2S

One of the outstanding unsolved problems in planetary science is the identification of the colored material in Jupiter's clouds. Thermochemical equilibrium calculations do not predict colored condensates in the observable levels of Jupiter's atmosphere (Lewis, 1969b), and remote spectroscopic observations are not likely to reveal the identity of the coloring agents directly. The significance of this gap in our understanding of Jupiter's atmospheric chemistry lies not only in the unknown nature of the chromophores themselves, but includes the nonequilibrium chemical reactions that produce them. In attempts to explain the colors, three different chemical systems have been studied in considerable theoretical and experimental detail: reactions involving sulfur-bearing materials; reactions involving phosphorous-bearing compounds; and the synthesis of organic polymers. Prinn and Owen (1976) present an excellent review of these studies. Only one molecule identified on Jupiter, PH_3, has a plausible, direct link to the production of a colored condensate (elemental red phosphorous) by photolysis. This process may be responsible for some of Jupiter's red coloration, especially that in the Great Red Spot (Prinn and Lewis, 1975), and possibly for the yellow and orange materials that color Jupiter's clouds on a global scale (Noy et al., 1981). Among alternative choices, elemental sulfur and polysulfides provide the appropriate spectrum of colors. The key observation for inferring their role in the clouds is the abundance and distribution of H_2S in Jupiter's atmosphere.

The search for H_2S on Jupiter has a long history, summarized in Table I. All entries are upper limits derived from analyses of spectroscopic data covering uv to mm wavelengths. Note that these measurements depended significantly upon special observing facilities. The wide range of sensitivities evident in this compilation is a consequence of the atmospheric level probed, the spectral resolution achieved, and the strength of the H_2S transition available for analysis. In general, the uv measurements set the most stringent limits to H_2S on Jupiter, but they apply only to stratospheric levels where H_2S should be severely depleted by photodissociation. Observations of planetary thermal emission from deeper tropospheric levels are possible for $\lambda \gtrsim 5$ μm. In fact, Bezard et al. (1983) concluded that supersaturated H_2S distributions are consistent with mm-wave thermal data and Voyager spectra at 8.5 μm. Confirmation of this result could in principle be made in Jupiter's 5-μm spectral window where holes in the lower clouds permit very sensitive searches for trace constituents in the deep troposphere. Unfortunately, the excellent planetary spectra available in this wavelength region (e.g. Kunde et al., 1982 for Voyager results; Larson et al., 1977 for airborne spectra; and Beer, 1975 for ground-based data) are of little help because no significant H_2S absorption occurs across this planetary window. The ν_2 fundamental of H_2S is at 8.45 μm, well above the 5-μm window, and the ν_1 and ν_3 modes are both near 3.8 μm and are completely obscured by Jovian CH_4 and NH_3. Moreover, there are no overtone or simple combination bands of H_2S in the 5-μm region. Thus, the 5-μm limit to H_2S in Table I is the least sensitive of all entries, since Treffers et al. (1978). had to use a very weak, unassigned H_2S band for their analysis. Opportunities elsewhere in the near-ir include the $\nu_1+\nu_2+\nu_3$ band accessible in ground-based observations at 1.6 μm, the $\nu_1+\nu_2$ and $\nu_2+\nu_3$ bands at 2.7 μm, and the $2\nu_1$, $2\nu_3$ and $\nu_1+\nu_3$ bands coincident with the Jovian window at 2 μm. We present below

TABLE I. Upper Limits to H_2S in Jupiter's Atmosphere

Upper Limit							
Abundance (cm-am)	Mixing Ratio	Atmospheric Level	Spectral Region (cm^{-1})	Type of Band	Spectral Resolution (cm^{-1})	Observing Facility	Reference
$3x10^{-3}$	$2.5x10^{-9}$	stratosphere	40000	electronic	~1120	Rocket	Greenspan and Owen, 1967
25	$1.3x10^{-5}$	upper troposphere	6250	(1,1,1)	10	UAO 1.5m	Cruikshank and Binder, 1969
$3x10^{-3}$	$6.0x10^{-9}$	stratosphere	40000	electronic	400	OAO	Owen and Sagan, 1972
3	$1.2x10^{-6}$	upper troposphere	6250	(1,1,1)	0.09	Palomar 5m	Owen et al., 1977
500	$5.0x10^{-5}$	lower troposphere	2000	?	0.6	KAO	Treffers et al., 1978
$5x10^{-4}$	$5.0x10^{-9}$	stratosphere	63000	electronic	400	IUE	Owen et al., 1980
--	$3.0x10^{-5}$	lower troposphere	2-15	(0,0,0)	$\gtrsim$3	various ground-based	Bézard et al., 1983
--	$3.0x10^{-5}$	upper troposphere	1200	(0,1,0)	4.3	Voyager	Bézard et al., 1983
0.1	$3.3x10^{-8}$	upper troposphere	3800	(1,1,0)(0,1,1)	0.1	KAO	This work

our analysis of the 2.7-μm H_2S spectrum; use of the 2-μm H_2S bands is dependent upon future acquisition of high resolution airborne spectra of Jupiter.

H_2S upper limit determination. We used the same two methods to search for H_2S that we employed in our Jovian H_2O analysis in Section III: a line-by-line search, and cross-correlation analysis. In Fig. 7 we display some of the spectral data used in our analysis. A typical laboratory comparison spectrum at the top of Fig. 7 illustrates the character of the $\nu_1+\nu_2$ and $\nu_2+\nu_3$ H_2S bands in the 2.7-μm region. These data originally contained numerous interfering H_2O lines because our optical path included several meters of laboratory air. Weak H_2O features were removed by the ratio spectrum technique; gaps in the spectrum mark the positions of saturated H_2O lines. Consequently, we lost a portion of the 2.7-μm H_2S spectrum, but we are confident that all prominent features left in Fig. 7 are produced by H_2S alone. Moreover, the same H_2O transitions that obscured these laboratory measurements also interfered with the planetary observations from the KAO. Thus, the ratio spectrum of Jupiter in Fig. 7 has similar gaps where telluric absorptions in the lunar comparison spectrum rendered the ratio calculation indeterminate.

The section of Jupiter's spectrum plotted in Fig. 7 offers the best chances for seeing individual H_2S lines. Telluric CO_2 and H_2O lines are very strong below 3740 cm^{-1}, and Jovian CH_4 saturates above 3800 cm^{-1}. To aid the reader in visualizing this search we plotted the planetary and laboratory spectra in Fig. 7 on absolute vacuum wavenumber scales (i.e. planetary Doppler shift removed, all corrections applied for non-standard spectroscopic air during the experiments). Some coincidences do appear, such as at 3767.2 and 3793.2 cm^{-1}. Other H_2S features, particularly the very strong lines at 3745.8 and 3792.9 cm^{-1}, do not match with absorptions in Jupiter's spectrum. We conclude that even a casual comparison of the spectra in Fig. 7 shows that there cannot be

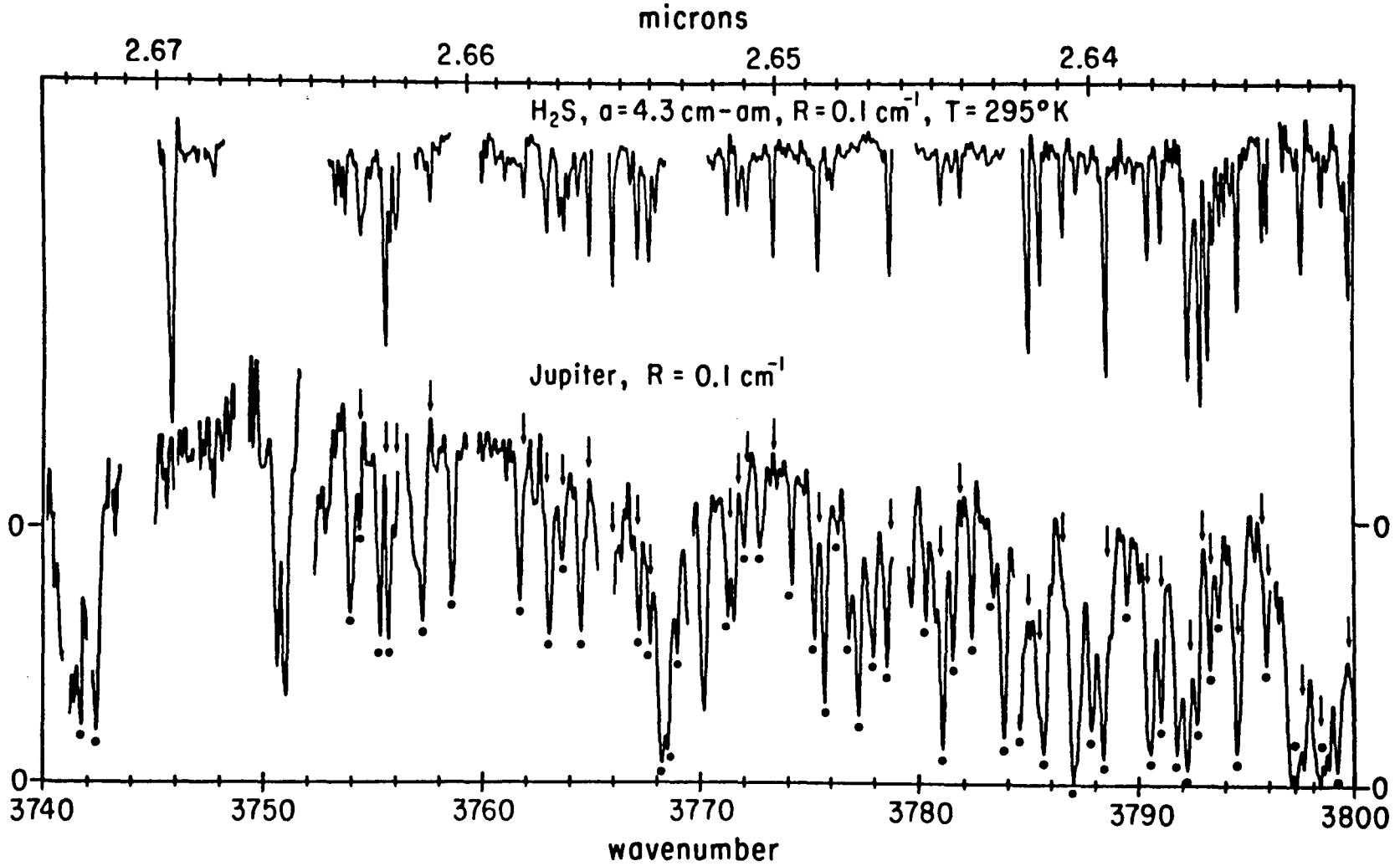
microns
2.67
2.66
2.65
2.64
H2S, a=4.3 cm-am, R=0.1 cm-1, T=295°K
Jupiter, R = 0.1 cm-1
0
0
0
0
3740
3750
3760
3770
3780
3790
3800
wavenumber

Figure 7

as much as 4.3 cm-am of H_2S in Jupiter's 2.7-μm spectrum. From our more detailed examination of these data, including spectral regions not plotted in Fig. 7, we made the following observations.

1. Every Jovian absorption in Fig. 7 that coincided with a strong H_2S line also matched a prominent line in our long path laboratory spectra of CH_4. In all cases we accepted the CH_4 assignment as more likely. The line position measurements are summarized in Table II for the spectral interval covered in Fig. 7. The absolute precision in the positions of isolated lines is about $\pm 5 \times 10^{-3}$ cm^{-1}, using H_2O lines as internal standards. However, so many laboratory and planetary features overlap that we report and compare all lines only to 5 figures. Furthermore, we regarded as a potential match any coincidences within about $\pm$ 0.1 cm^{-1}.

2. In spectral regions where there are fewer strong CH_4 lines, we found no coincidences of strong H_2S lines with planetary absorptions. The best example is at 3745.8 cm^{-1} where the strongest feature in the 2.7-μm spectrum of H_2S coincides with a narrow region of the Jovian continuum displaying only noise introduced by complex telluric absorptions in the ratio calculation. From such lines we concluded that amounts of H_2S as high as 4.3 cm-am were incompatible with Jupiter's 2.7-μm spectrum.

3. To test for H_2S using all positional information simultaneously, we cross-correlated the planetary and laboratory data as previously described in Section III in our search for Jovian H_2O. We saw no Doppler-shifted signature of H_2S. However, the strong correlation of telluric and laboratory H_2O could have masked more subtle indications of Jovian H_2S. To maximize the sensitivity of this numerical procedure we removed all H_2O lines from our H_2S data by an interactive graphics editing procedure. The resulting spectrum was similar to that at the top of Fig. 7, with flat continua bridging the gaps to provide a continuous file for computations. This correlogram also failed

TABLE II. Possible Assignments to Jovian Absorption Lines in the 3750-3800 cm^{-1} Region

Jupiter (cm^{-1})	H_2S (cm^{-1})	CH_4 (cm^{-1})	Jupiter (cm^{-1})	H_2S (cm^{-1})	CH_4 (cm^{-1})
3750.71	--	--	3777.23	--	3777.15
3751.07	--	--	3777.93	--	3777.86
3754.04	--	3754.00	3778.54	--	3778.56
3754.44	--	3754.43	3779.62	--	--
3755.36	--	3755.37	3780.30	--	3780.32
3755.73	3755.67	3755.70	3780.73	--	3780.71
3757.30	--	3757.27	3781.04	3781.11	3781.03
3758.65	--	3758.67	3781.50	3781.61	3781.53
3761.73	--	3761.76	3782.36	--	3782.33
3762.39	--	3762.41	3783.35	--	3783.37
3763.08	3763.07	3763.02	3783.81	--	3783.82
3763.66	--	3763.60	3785.64	3785.57	3785.60
3764.50	3764.51	3764.50	3786.95	--	3787.02
3767.21	3767.21	3767.19	3787.81	3787.77	3787.88
3767.72	3767.80	3767.71	3788.33	--	3788.30
3768.22	3768.10	3768.25	3789.41	--	3789.30
3768.50	--	3768.54	3789.97	--	3789.92
3768.95	--	3768.99	3790.46	3790.49	3790.55
3770.18	3770.17	3770.10	3790.93	--	3790.99
3771.28	3771.40	3771.40	3791.70	--	3791.76
3771.56	--	--	3792.16	--	3792.09
3772.03	--	3772.07	3792.60	--	3792.58
3772.76	--	3772.74	3793.20	3793.24	3793.19
3774.21	--	3774.26	3793.61	3793.50	3793.57
3775.24	--	3775.25	3794.48	--	3794.52
3775.70	--	3775.73	3795.30	--	--
3776.80	--	3776.83	3795.80	3795.77	3795.80

to show an extremum at the position of Doppler-shifted planetary lines. We concluded that the entire pattern of H_2S lines at 2.7 μm was incompatible with Jupiter's spectrum.

4. Certain prominent H_2S lines, such as at 3745.8 cm^{-1} and the group near 3792 cm^{-1}, are apparently low-J transitions whose intensities will not be susceptible to strong temperature effects. We used such lines to set quantitative limits to the abundance of H_2S on Jupiter.

5. Using H_2S spectra at lower abundances than in Fig. 7 we determined that about 0.25 cm-am would produce equivalent widths in the strongest H_2S lines at the noise level of the planetary data. We adopted this value as our upper limit to H_2S on Jupiter: $\eta a \sim 0.25$ cm-am. The one-way transmission is ~ 0.1 cm-am for an air mass $\eta = 2.5$. The corresponding upper limit to the H_2S mixing ratio is $\sim 3.3 \times 10^{-8}$ and the limit to the elemental abundance [S]/[H] is $\sim 1.7 \times 10^{-8}$, about 10^{-3} times the solar value of 1.9×10^{-5} (Cameron, 1982).

Discussion. Our upper limit to sulfur in Jupiter's atmosphere is the most stringent observational limit applicable to tropospheric levels (see Table I). We use this limit in the discussion below to constrain possible roles for sulfur-bearing constituents in Jupiter's atmosphere. In Fig. 8 we show several predicted distributions of H_2S, each emphasizing a specific depletion mechanism using a simplified chemical model. Our presentation closely parallels that of Bezard et al. (1983), but our conclusions differ significantly. In all cases we assume that a solar [S]/[H] abundance applies below the main cloud deck and that the dominant sulfur-bearing species in Jupiter's atmosphere for levels $T \geq 300°K$ is H_2S (Barshay and Lewis, 1978).

Curve A, a constant H_2S mixing ratio, assumes no significant depletion of gaseous H_2S in the atmospheric transport cycle. This distribution must be

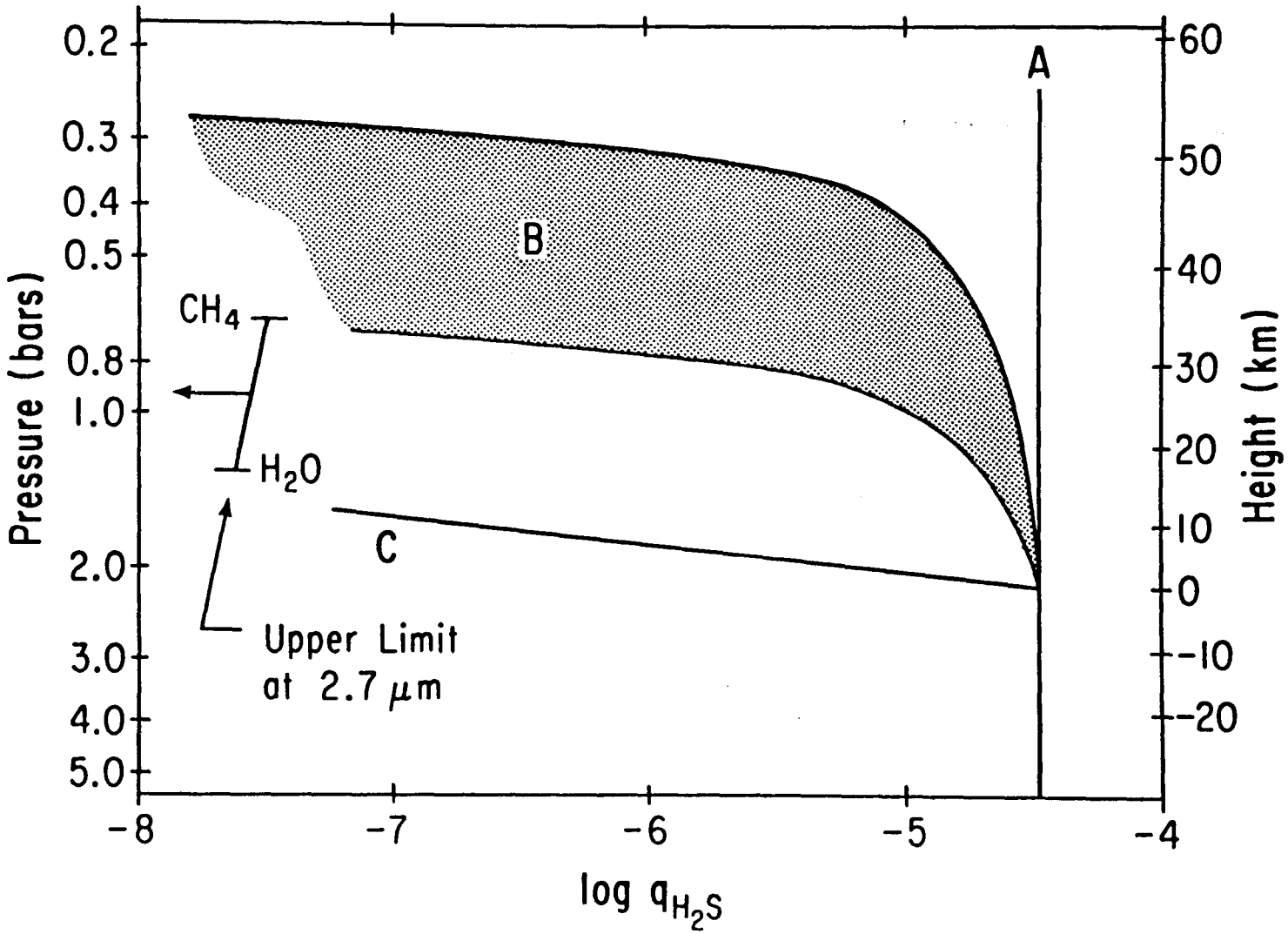
0.2
0.3
0.4
0.5
0.8
1.0
2.0
3.0
4.0
5.0
Pressure (bars)
60
50
40
30
20
10
0
-10
-20
Height (km)
A
B
C
CH4
H2O
Upper Limit
at 2.7 μm
-8
-7
-6
-5
-4
log qH2S

Figure 8

considered for two reasons. First, other chemically active Jovian constituents (e.g. PH_3, GeH_4) do survive passage through atmospheric levels where, under equilibrium conditions, chemical reactions should have reduced their abundances to spectroscopically undetectable amounts. Second, it is not cold enough anywhere in Jupiter's atmosphere for solid H_2S to form. From the International Critical Tables (1928) the vapor pressure of H_2S above crystalline ice is

$$P_{H_2S} = 10^{(-\frac{1081}{T}+7.78)}/760 \qquad (1)$$

where T is the temperature (°K). In the cold trap at the tropopause (P ~0.12 bar, T ~110°K), the vapor pressure P_{H_2S} is 1.5×10^{-5} bars. Since this is larger than the maximum partial pressure (3.6×10^{-6} bar) of H_2S at the tropopause (e.g. for [S]/[H] = 1.6×10^{-5}), solid H_2S will not condense at this coldest location in Jupiter's atmosphere nor in warmer levels above and below it. Thus, the distribution of gaseous H_2S in Curve A projects through the upper cloud layer into the stratosphere. The upper end of distribution A is incompatible with upper limit measurements at many wavelengths (see Table I), but Bezard et al. (1983) proposed that Curve A applies to at least some mid-tropospheric levels between the cloud layers, a condition they called supersaturated.

Curves occupying area B in Fig. 8 model depletion of H_2S above the main cloud deck through photodissociation by solar uv photons. Specific distributions such as the two extreme curves defining area B are numerical solutions of the steady state continuity equation,

$$\frac{d\Phi}{dz} = -Lnq_{H_2S} \qquad (2)$$

where Φ is the H_2S flux, L is the H_2S loss rate by photolysis, n is the number density of the background atmosphere, and q_{H_2S} is the height-dependent H_2S mixing ratio. For the tropospheric levels considered here, the vertical transport of H_2S can be expressed as,

$$\Phi = -Kn\frac{dq_{H_2S}}{dz} \qquad (3)$$

where K is the eddy diffusion coefficient. In our computations we used height-dependent values of L for H_2S photolysis from Visconti (1981) and both constant (10^5-10^9 cm^2/sec) and height-dependent (e.g. scale height $\sim$ 20 km) expressions for K. In general, all distributions show relatively little H_2S depletion between the cloud layers and very rapid depletion in and above the upper clouds. Although different choices of L and K change the H_2S distributions within area B, the variations are not diagnostic and will not be discussed further. The extreme curves defining area B represent H_2S distributions at the base of the upper cloud layer and in the region above these clouds. Of course, distributions outside area B could be considered for different choices of boundary conditions. Our assumptions were, (1) good observational limits to H_2S in the upper troposphere and stratosphere establish the upper bound to area B, and (2) stratospheric aerosols and the upper clouds prevent significant penetration of solar uv photons below the upper clouds, thus defining the lower boundary to area B.

Curve C models the depletion of H_2S by reaction with NH_3 to form NH_4SH, a white crystalline solid that may constitute the bulk of the lower cloud mass. Under equilibrium conditions the reaction

$$NH_4SH(s) \rightleftarrows NH_3(g) + H_2S(g) \qquad (4)$$

very effectively removes H_2S from Jupiter's atmosphere with a scale height of just a few km (Prinn and Owen, 1975). We review this prediction using Bjoraker's revised atmospheric parameters for the lower troposphere. From the equilibrium constant k for the reaction in (4),

$$k = P_{NH_3} P_{H_2S} \tag{5a}$$

$$\log_{10} k = 14.82 - 4705/T \text{ (Lewis, 1969a)} \tag{5b}$$

we obtain

$$\log_{10} P_{H_2S} = 14.82 - 4705/T - \log_{10} P_{NH_3} \tag{6}$$

where P denotes the partial pressure (bars) of the reactants in atmospheric layers specified by the temperature T (°K). We summarize in Table III the predicted abundances of H_2S in the formation region of Jupiter's clouds. The values of q_{H_2S} indicate that the base of the NH_4SH cloud is near P=2.1 bars, T=210°K, and that the scale height for such condensation is $\sim$ 2 km, not substantially different from previous calculations.

The actual distribution of H_2S in Jupiter's atmosphere may not adhere strictly to any one of the three types of distributions plotted in Fig. 8. Possible deviations include: (1) the equilibrium condensation represented by Curve C may overestimate the efficiency of H_2S depletion by cloud formation, since knowledge of the complementary physical processes is not well understood; (2) the photolysis of H_2S given by area B may underestimate the efficiency of H_2S depletion between the cloud layers, especially in areas where the upper cloud layer is thin or absent; and (3) rapid vertical transport may produce H_2S distributions not considered in Fig. 8 because they require simultaneous inclusion of several depletion mechanisms. Within these limitations we now relate our observed H_2S upper limit to the predictions in Fig. 8.

We present our abundance limit to H_2S in Fig. 8 as the range of mixing ratios that corresponds to the probable pressure levels at the base of the 2.7-μm spectral line forming region (0.75 bar from CH_4, 1.2 bars from H_2O). From simple inspection of the location of our result with respect to distributions A, B, and C, we note that:

1. Our upper limit is irreconcilable with Curve A for all atmospheric levels above the base of the upper cloud layer. Significant depletion of H_2S apparently occurs in Jupiter's deeper troposphere.

2. Our result eliminates a major role for H_2S photolysis above the upper clouds (most of area B in Fig. 8) because the predicted H_2S distributions could have been detected at our sensitivity limits. This mechanism is marginally compatible with the observations at the very base of the upper cloud layer since the upper limit to H_2S coincides with the lower limit to area B in Fig. 8. However, independent evidence (see Section V) argues against H_2S photolysis at such levels because of the lack of solar uv flux. These results therefore suggest that significant H_2S photolysis does not occur anywhere in the vicinity of Jupiter's upper cloud layers.

3. On the assumption that a reservoir of H_2S exists immediately below the main cloud deck, our limit demonstrates that chemical depletion has very efficiently destroyed this species within a vertical distance of 25 km or less.

4. Our upper limit is most compatible with the NH_4SH condensation model, in the sense that distribution C is below our H_2S detection threshold.

We consider the implications of these results in the next section.

V. CONCLUSIONS

The results of our spectral analyses in the preceeding sections support the following conclusions concerning Jupiter's atmospheric chemistry.

Height dependence of solar flux in Jupiter's lower troposphere. The photo-chemical processing of sulfur-bearing compounds in Jupiter's atmosphere

TABLE III. Equilibrium Distribution of H_2S

$z^{(1)}$ (km)	$p^{(1)}$ (bars)	$T^{(1)}$ (°K)	$P_{NH_3}{}^{(1)}$ (bars)	$P_{H_2S}{}^{(2)}$ (bars)	$q_{H_2S}{}^{(3)}$	Comments
105	0.80	154	2.1×10^{-4}	1.0×10^{-12}	1.2×10^{-12}	Base of upper cloud layer
100	0.98	164	2.5×10^{-4}	6.4×10^{-11}	6.5×10^{-11}	
95	1.17	174	3.0×10^{-4}	2.3×10^{-9}	2.0×10^{-9}	
90	1.39	184	3.6×10^{-4}	5.6×10^{-8}	4.0×10^{-8}	Upper limit to H_2S at 2.7 μm
85	1.64	194	4.3×10^{-4}	9.4×10^{-7}	6.0×10^{-7}	
83	1.75	198	4.6×10^{-4}	2.6×10^{-6}	1.5×10^{-6}	
81	1.86	202	4.8×10^{-4}	7.0×10^{-6}	3.8×10^{-6}	
79	1.97	206	5.1×10^{-4}	1.7×10^{-5}	8.8×10^{-6}	NH_4SH cloud
77	2.10	210	5.4×10^{-4}	4.5×10^{-5}	2.1×10^{-5}	Condensation of NH_4SH begins
75	2.22	214	5.8×10^{-4}	6.7×10^{-5}	3.3×10^{-5}	[S]/[H] constrained to solar value below this level
28	7.00	301	1.8×10^{-3}	2.3×10^{-4}	3.3×10^{-5}	Base of 5-μm spectral line forming region
0	12.00	353	3.1×10^{-3}	4.0×10^{-4}	3.3×10^{-5}	Base of tropospheric model

(1) Atmospheric parameters from Bjoraker (1984)

(2) Calculated from Eq. 6.

(3) $q_{H_2S} = P_{H_2S}/P$ = mole fraction of H_2S.

depends upon the degree to which solar uv flux penetrates into the relatively clear area between the cloud layers. Two processes, photolysis of H_2S and photodissociation of sulfur-bearing condensates in the lower cloud mass, have been studied to explain Jupiter's visible colors (Prinn, 1970; Lewis and Prinn, 1970; Prinn and Owen, 1976). We do not believe that either process controls Jupiter's sulfur chemistry, a conviction based upon our upper limit to H_2O at 2.7 μm. To support this conclusion we invoke the reasonable assumption that wherever uv photons penetrate the Jovian haze and cloud layers, ir photons will do so even more efficiently because of reduced scattering losses. Thus, if solar uv photons penetrate to the lower cloud tops, the accompanying ir flux would show obvious absorption by Jovian H_2O. Bjoraker's predicted H_2O abundances near the lower cloud tops are in the range of 1-5 μm precipitable H_2O (Bjoraker, 1984), amounts readily detectable by simple visual inspection of our high resolution planetary spectrum (see Fig. 5 and its discussion in Section III). However, our negative search for Jovian H_2O at 2.7 μm rules out significant solar ir flux between the cloud layers, and it is therefore unlikely that substantial uv flux exists in Jupiter's lower troposphere. This result conflicts with some other two-cloud models of Jupiter's atmosphere (e.g. Sato and Hansen, 1979), but we note that our conclusion based upon new high resolution airborne ir spectra is consistent with other recent studies using such diverse techniques as uv photometry from Voyager (Hord et al., 1979) and visible polarimetry from Pioneer (Smith and Tomasko, 1984). Hord et al. conclude that solar uv photons ($\lambda \sim 2400$ Å) probably do not penetrate Jupiter's upper clouds because of the combined effectiveness of such high altitude extinction sources as conservative Rayleigh scattering ($\tau \sim 2$ at 0.6 bar), absorbing aerosols distributed between 0.05-0.375 bar, and a high uv optical thickness ($\tau \sim 5$) for the upper cloud itself. Smith and Tomasko report that spatially-resolved polarization measurements in blue light do not reveal any spots that could be associated with

cloud-free areas in the belts. They conclude that a cloud with $\tau \sim 1.5$ exists over both belts and zones at the 0.32 bar level. Thus, photolytic reactions in Jupiter's lower troposphere may not be as significant as was previously thought.

Cloud chromophores. In Section IV we noted that our upper limit to H_2S on Jupiter eliminated a major role for H_2S photolysis above the base of the upper clouds. Our discussion, above, concerning the height dependence of solar photons in Jupiter's atmosphere argues against H_2S photolysis between the cloud layers. These two results imply that there is no location in the spectroscopically accessible regions of Jupiter's atmosphere where colored, sulfur-bearing condensates can be photochemically generated in significant amounts. This surprising reversal of historical expectations leaves just two other chemical systems (phosphorous-bearing condensates, organic polymers) as primary candidates for explaining Jupiter's visible coloration. Available data support at least a partial role for phosphorous as a cloud chromophore (Lewis and Prinn, 1975; Noy et al., 1981). Further progress in identifying specific compounds is likely to be slow because of the iterations required between observational work, laboratory simulations, and theoretical modeling.

Cloud composition. The association of Jupiter's upper clouds with NH_3 and the lower clouds with NH_4SH is a consequence of thermochemical predictions (Lewis, 1969a) rather than spectroscopic detections. The existence of the lower cloud is required by thermal models, and its composition is convincingly specified by thermochemical equilibrium models. The substantial depletion of H_2S in Jupiter's lower troposphere implies that Jupiter's solar complement of sulfur has been converted to other compounds. In connection with the last point, we noted in Section IV that our limit to the H_2S mixing ratio was most compatible with distribution C in Fig. 8, the cloud-forming NH_4SH condensation model. That is, this mechanism alone could deplete the H_2S abundance on Jupiter to below our detection threshold, in effect, locking up so much of Jupiter's sulfur that

a negligible amount is left for convection to higher altitudes to participate in photochemical processes. In the absence of any competing model, we conclude that our analysis of the abundance and distribution of H_2S in Jupiter's atmosphere contributes strong new circumstantial evidence that NH_4SH is the primary component in the lower cloud layer.

We also called attention in Section III to possible signatures of NH_3 ice in our low resolution version of Jupiter's 2.7-μm spectrum. If these features can be simulated with detailed modeling, they may eventually constitute direct spectroscopic proof that solid NH_3 is the principal component in the upper cloud layer.

Global abundance of sulfur in Jupiter. Throughout our analysis and discussion there were many opportunities to qualify our results because of uncertainties in the observations, the laboratory data, or the theoretical models. We could not address in detail all problems, but we call attention here to one assumption that, if inappropriate, will invalidate many of our conclusions. We consistently assumed that the Jovian [S]/[H] value is solar immediately below the lower cloud deck. It is customary to adopt the solar abundances of the elements for modeling the interior of Jupiter (Lewis, 1969b), but there could have been events during this planet's evolution that altered an initially solar distribution. This possibility was taken seriously (Podolak, 1977) when the first spectroscopic determination of [O]/[H] on Jupiter was only $\sim 10^{-3}$ times the solar value (Larson et al., 1975), a discrepancy that is still not resolved by meteorological arguments alone (Bjoraker, 1984). In analogy with this situation we therefore conclude with the speculation that an alternate explanation of our low limit to H_2S on Jupiter is simply that [S]/[H] is significantly depleted in this planet's interior.

ACKNOWLEDGEMENTS

We express our special thanks to the administrative and technical staff of the Kuiper Airborne Observatory for their assistance during our 1982 flight program. We are grateful for useful discussions with M. Tomasko and J. Lewis. RH thanks the Max Planck Institute for supporting him as a visiting scientist at the Lunar and Planetary Laboratory and GLB acknowledges his support from NASA's Graduate Student Researchers Program. The airborne spectroscopy project is funded by NASA grant NGR 03-002-332.

References

Barshay, S. S., and J. S. Lewis (1978). Chemical structure of the deep atmosphere of Jupiter. Icarus 33, 593-611.

Beer, R. (1975). Detection of carbon monoxide in Jupiter. Astrophys. J. 200, L167-L169.

Bezard, B., J. P. Baluteau, and A. Marten (1983). Study of the deep cloud structure in the equatorial region of Jupiter from Voyager infrared and visible data. Icarus 54, 434-455.

Bjoraker, G. L. (1984). Ph. D. dissertation, Lunar and Planetary Laboratory, The University of Arizona, in preparation.

Cameron, A. G. W. (1982). Elemental and nuclidic abundances in the solar system. In Essays in Nuclear Astrophysics (C. A. Barnes, D. D. Clayton, and D. N. Schramm, eds.), pp. 23-43. Cambridge University Press, Cambridge, England.

Cruikshank, D. P. and A. B. Binder (1969). Minor constituents in the atmosphere of Jupiter. Astrophys. Space Sci. 3, 347-356.

Danielson, R. E. (1966). The infrared spectrum of Jupiter. Astrophys. J. 143, 949-960.

Danielson, R. E., and M. G. Tomasko (1969). A two-layer model of the Jovian clouds. J. Atmos. Sci. 26, 889-897.

Davis, D. S., H. P. Larson, M. Williams, G. Michel, and P. Connes (1980). Infrared Fourier spectrometer for airborne and ground-based astronomy. Appl. Opt. 19, 4138-4155.

de Bergh, C., J. P. Maillard, J. Lecacheux, and M. Combes (1976). A study of the $3\nu_3$-CH_4 region in a high-resolution spectrum of Jupiter recorded by Fourier transform spectroscopy. Icarus 29, 307-210.

Drossart, P., and T. Encrenaz (1983). The Jovian spectrum in the 3-μm window. Icarus 55, 390-398.

Ferraro, J. R., and U. Fink (1977). Near infrared reflectance spectra and analysis of H_2S frost as a function of temperature. J. Chem. Phys. 67, 409-413.

Fink, U., and H. P. Larson (1979). The infrared spectra of Uranus, Neptune and Titan from 0.8 to 2.5 microns. Astrophys. J. 233, 1021-1040.

Greenspan, J. A., and T. Owen (1967). Jupiter's atmosphere: its structure and composition. Science 156, 1489-1494.

Hord, C. W., R. A. West, K. E. Simmons, D. L. Coffeen, M. Sato, A. L. Lane, and J. T. Bergstrahl (1979). Photometric observations of Jupiter at 2400 Angstroms. Science 206, 956-959.

International Critical Tables (1928). McGraw-Hill, New York.

Kunde, V., R. Hanel, W. Maguire, D. Gautier, J. P. Baluteau, A. Marten, A. Chedin, N. Husson, and N. Scott (1982). The tropospheric gas composition of Jupiter's North Equatorial Belt (NH_3, PH_3, CH_3D, GeH_4, H_2O) and the Jovian D/H isotopic ratio. Astrophys. J. 263, 443-467.

Larson, H. P., U. Fink, R. Treffers, and T. N. Gautier (1975). Detection of water vapor on Jupiter. Astrophys. J. 197, L137-L140.

Larson, H. P., R. R. Treffers, and U. Fink (1977). Phosphine in Jupiter's atmosphere: the evidence from high altitude observations at 5 microns. Astrophys. J. 211, 972-979.

Lewis, J. S. (1969a). The clouds of Jupiter and the NH_3-H_2O and NH_3-H_2S systems. Icarus 10, 365-378.

Lewis, J. S. (1969b). Observability of spectroscopically active compounds in the atmosphere of Jupiter. Icarus 10, 393-401.

Lewis, J. S., and R. G. Prinn (1970). Jupiter's clouds: structure and composition. Science 169, 472-473.

Lutz, B. L., T. Owen, and R. D. Cess (1976). Laboratory band strengths of methane and their application to the atmospheres of Jupiter, Saturn, Uranus, Neptune, and Titan. Astrophys. J. 203, 541-551.

Marten, A., D. Rouan, J. P. Baluteau, D. Gautier, B. J. Conrath, R. A. Hanel, V. Kunde, and R. Samuelson (1981). Study of the ammonia ice cloud layer in the equatorial region of Jupiter from the infrared interferometric experiment on Voyager. Icarus 46, 233-248.

Noy, N., M. Podolak, and A. Bar-Nun (1981). Photochemistry of phosphine and Jupiter's Great Red Spot. J. Geophys. Res. 86, 11985-11988.

Owen, T., and C. Sagan (1972). Minor constituents in planetary atmospheres: ultraviolet spectroscopy from the Orbiting Astronomical Observatory. Icarus 16, 557-568.

Owen, T., A. R. W. McKellar, T. Encrenaz, J. Lecacheux, C. de Bergh, and J. P. Maillard (1977). A study of the 1.56μ NH_3 band on Jupiter and Saturn. Astron. Astrophys. 54, 291-295.

Owen, T., J. Caldwell, A. R. Rivolo, V. Moore, A. L. Lane, C. Sagan, G. Hunt, and C. Ponnamperuma (1980). Observations of the spectrum of Jupiter from 1500 to 2000 Å with the IUE. Astrophys. J. 236, L39-L42.

Owen, T., and R. J. Terrile (1981). Colors on Jupiter. J. Geophys. Res. 86, 8797-8814.

Podolak, M. (1977). The abundance of water and rock in Jupiter as derived from interior models. Icarus 30, 155-162.

Prinn, R. G. (1970). UV radiative transfer and photolysis in Jupiter's atmosphere. Icarus 13, 424-436.

Prinn, R. G., and J. S. Lewis (1975). Phosphine on Jupiter and implications for the Great Red Spot. Science 190, 274-276.

Prinn, R. G., and T. Owen (1976). Chemistry and spectroscopy of the Jovian atmosphere. In Jupiter (T. Gehrels, Ed.), pp. 319-371. Univ. of Arizona Press, Tucson, Arizona.

Ridgway, S. T., H. P. Larson, and U. Fink (1976). The infrared spectrum of Jupiter. In Jupiter (T. Gehrels, Ed.), pp. 384-417. Univ. of Arizona Press, Tucson, Arizona.

Sato, M., and J. E. Hansen (1979). Jupiter's atmospheric composition and cloud structure deduced from absorption bands in reflected sunlight. J. Atmos. Sci. 36, 1133-1167.

Sill, G., U. Fink, and J. R. Ferraro (1980). Absorption coefficients of solid NH_3 from 50 to 7000 cm^{-1}. J. Opt. Soc. Am. 70, 724-739.

Smith, P. H., and M. G. Tomasko (1984). Photometry and polarimetry of Jupiter at large phase angles. II. Polarimetry of the South Tropical Zone, South Equatorial Belt, and the Polar Regions from the Pioneer 10 and 11 missions. Icarus 57, 000-000.

Terrile, R. J., and J. A. Westphal (1977). The vertical cloud structure of Jupiter from 5 μm measurements. Icarus 30, 274-281.

Treffers, R. R., H. P. Larson, U. Fink, and T. N. Gautier (1978). Upper limits to trace constituents in Jupiter's atmosphere from an analysis of its 5-μm spectrum. Icarus 34, 331-343.

Visconti, G. (1981). Penetration of solar uv radiation and photodissociation in the Jovian atmosphere. Icarus 45, 638-652.

FIGURE CAPTIONS

Figure 1. A chronology of spectroscopic observations of Jupiter's atmospheric transmission window in the 2.7-μm region. (a) Balloon-borne data adapted from Danielson (1966) that originally revealed this region of transparency in Jupiter's atmosphere. Intensities are calibrated in terms of albedo. (b) Airborne observations showing details of Jovian CH_4 and NH_3 absorption across this window. Telluric absorptions and the instrumental response function have been removed from these data. (c) Excerpt from the new high resolution airborne spectrum showing many Doppler-resolved planetary CH_4 lines. No part of this planetary window at 2.7-μm is accessible in ground-based observations.

Figure 2. The lunar comparison spectrum in the 2.7-μm region from the Kuiper Airborne Observatory. (a) Overview showing the locations of the strong telluric H_2O and CO_2 absorptions that affect astronomical observations even at an altitude of 12.4 km. (b) High resolution detail at the center of a telluric CO_2 band. (c) High resolution detail in the region of strong telluric H_2O absorption. These spectra are uncorrected for instrument response. The Jovian 2.7-μm window is coincident with these telluric CO_2 and H_2O features. All intensities range from 0 to maximum on an uncalibrated, linear scale.

Figure 3. A comparison of Jupiter's spectral reflectivity in the 2.7-μm region with spectra of molecules known or suspected to be present in its atmosphere. The spectra of H_2, HD and HF were calculated from molecular parameters. The locations of spectral features of the more complex molecules in (f) were determined from short-path laboratory spectroscopy experiments. The comparison spectra of CH_4

and NH_3 were produced using the LPL 40-m White cell. All intensities range from 0 to maximum on an uncalibrated, linear scale. This composite demonstrates the scientific potential of studies of Jupiter's 2.7-μm window in spite of its narrow width and awkward location with respect to telluric absorptions.

Figure 4. Schematic illustration of Jupiter's vertical atmospheric structure based on the thermal model of Bjoraker (1984). Arrows indicate the direction of atmospheric convection and the locations of cloud-forming regions. The values of the optical thickness parameter τ are appropriate only for the one-way transmission of thermal emission at 5 μm. In general, higher values of τ are required at shorter wavelengths. The spectral line forming region at 2.7 μm was established by the observed abundances of CH_4 and H_2O in Jupiter's high resolution spectrum. This level is just below the base of the upper cloud layer, deeper than at shorter wavelengths but significantly higher than at 5 μm.

Figure 5. An illustration of the search for Jovian H_2O in the 2.7-μm region. (a) A section of Jupiter's high resolution in which conditions are good for seeking Doppler-shifted planetary H_2O lines accompanying the telluric lines. (b) A section of the lunar comparison spectrum that contains the prominent telluric H_2O line at 3759.8 cm^{-1}. (c) A section from the synthetic spectrum of H_2O fit to the lunar comparison spectrum in (b). This synthetic spectrum contains a Doppler-shifted component to illustrate the appearance of Jovian H_2O if it existed at 2.7 μm with an abundance near 1 μm precipitable H_2O. Simple comparisons of the shapes of the 3759.8 cm^{-1} line profile in (a), (b), and (c) are sufficient to exclude this amount of H_2O on Jupiter at 2.7 μm. All intensities range from 0 to maximum on an uncalibrated, linear scale.

Figure 6. Correlograms used in the search for Jovian H_2O. The vertical scale indicates the degree of correlation in arbitrary units. (a) The cross-correlation of Jupiter's high resolution spectrum with the synthetic spectrum of H_2O fit to the lunar comparison spectrum. (b) The cross-correlation of the high altitude lunar comparison spectrum with the synthetic spectrum of H_2O. (c) Autocorrelation of the synthetic spectrum of H_2O. (d) Cross-correlation of two synthetic spectra of H_2O, each fit to the high altitude lunar comparison spectrum but with one containing a hypothetical Doppler-shifted planetary component. The similarity of the correlograms in (a), (b), and (c), compared to the obvious broadening of the correlogram in (d) by the planetary component, demonstrates that the Jovian H_2O abundance at 2.7 μm must be substantially less than 1 μm precipitable H_2O.

Figure 7. A section of Jupiter's high resolution ratio spectrum in which the search for H_2S is optimized. Gaps in this spectrum occur in regions of strong telluric H_2O absorption. The broader gaps in the laboratory comparison spectrum of H_2S are due to even more serious obscuration by H_2O in our laboratory experiments. The solid circles mark the positions of prominent CH_4 lines revealed in our long-path laboratory spectra, and the arrows locate the positions of the H_2S features displayed above them. A cross-correlation of these two spectra, which contain no H_2O lines, showed only noise at the location for Doppler-shifted Jovian H_2S. Intensities range from 0 to maximum on an uncalibrated, linear scale.

Figure 8. Predicted vertical distributions of H_2S in Jupiter's atmosphere. (A) Constant mixing ratio for a solar [S]/[H] abundance. (B) Area occupied by distributions controlled by photolysis. The upper

boundary is set by observed upper limits to H_2S, and the lower boundary is constrained by evidence that solar uv photons do not penetrate significantly below the base of the upper cloud layer. (C) Depletion of H_2S by condensation of NH_4SH to form the lower cloud layer. The upper limit to H_2S from Jupiter's 2.7-μm spectrum is located in this figure as the range of values (2.1×10^{-8}-3.3×10^{-8}) between the pressure levels (0.75-1.2 bars) given by the observed abundance of CH_4 and the upper limit to H_2O. This spread in values is one measure of the uncertainty in the H_2S upper limit measurement. In the text all values for the sulfur limit in Jupiter are referred to the atmospheric level given by the CH_4 abundance only.

1. Report No.	2. Government Accession No.	3. Recipient's Catalog No.
NASA TM-86661		

4. Title and Subtitle	5. Report Date
THE JOVIAN ATMOSPHERIC WINDOW AT 2.7 μm: A SEARCH FOR H_2S	November 1984
	6. Performing Organization Code

7. Author(s)	8. Performing Organization Report No.
Harold P. Larson,* D. Scott Davis,* Reiner Hofmann,† and Gordon L. Bjoraker*	85043
	10. Work Unit No.

9. Performing Organization Name and Address	11. Contract or Grant No.
*University of Arizona, Tucson, Ariz. 85721 †Max-Planck-Institut fur Physik und Astrophysik Institut fur Extraterrestriche Physik, 8046 Garching bei Munchen, Federal Republic of Germany	

12. Sponsoring Agency Name and Address	13. Type of Report and Period Covered
National Aeronautics and Space Administration Washington, D.C. 20546	Technical Memorandum
	14. Sponsoring Agency Code

15. Supplementary Notes

Preprint Series #25. Supported by NASA grants.
Point of Contact: L. C. Haughney, Ames Research Center, MS 211-12, Moffett Field, Calif. 94035 (415) 965-5339 or FTS 448-5339

16. Abstract

We have observed the atmospheric transmission window at 2.7 μm in Jupiter's atmosphere at a spectral resolution of 0.1 cm^{-1} from the Kuiper Airborne Observatory. From our analysis of the CH_4 abundance (~80 m-am) and the H_2O abundance (<0.0125 cm-am) we determined that the penetration depth of solar flux at 2.7 μm is near the base of the NH_3 cloud layer. Our upper limit to H_2O at 2.7 μm and other recent results suggest that photolytic reactions in Jupiter's lower troposphere may not be as significant as was previously thought. Our search for H_2S in Jupiter's atmosphere yielded an upper limit of ~0.1 cm-am. The corresponding limit to the element abundance ratio [S]/[H] was $\sim 1.7\times10^{-8}$, about 10^{-3} times the solar value. Upon modeling the abundance and distribution of H_2S in Jupiter's atmosphere we concluded that, contrary to expectations, sulfur-bearing chromophores are not present in significant amounts in Jupiter's visible clouds. Rather, it appears that most of Jupiter's sulfur is locked up as NH_4SH in a lower cloud layer. Alternatively, the global abundance of sulfur in Jupiter may be significantly depleted.

17. Key Words (Suggested by Author(s))	18. Distribution Statement
Planets: Jupiter Planetary: Atmosphere Spectroscopy: Near-Infrared	Unlimited Subject Category - 89

19. Security Classif. (of this report)	20. Security Classif. (of this page)	21. No. of Pages	22. Price*
Unclassified	Unclassified	38	A03

*For sale by the National Technical Information Service, Springfield, Virginia 22161

End of Document